Pergamon

Int. J. Heat Mass Transfer. Vol. 39, No. 7, pp. 1363–1378, 1996

0017–9310/96 $15.00 + 0.00

0017–9310(95)00225–1

Numerical study of double-diffusive natural convection in a porous cavity using the Darcy–Brinkman formulation

B. GOYEAU, J.-P. SONGBE and D. GOBIN

Fluides, Automatique et Systèmes Thermiques URA 871, Laboratoire de l'Université Pierre et Marie Curie associé au CNRS Campus Universitaire, Bât. 502, 91405 Orsay Cedex, France

(*Received* 23 *March* 1995 *and in final form* 16 *June* 1995)

Abstract—This paper deals with natural convection in confined porous media, driven by cooperating thermal and solutal buoyancy forces. The physical model for the momentum conservation equation makes use of the Brinkman extension of the classical Darcy equation, and the set of coupled equations is solved using a finite volume approach. The numerical simulations presented here span a wide range of the main parameters (the Rayleigh and Darcy numbers) in the domain of positive buoyancy numbers and for $Le > 1$. When possible, the results are compared with previous numerical data or existing scaling laws. The results are mainly analyzed in terms of the average heat and mass transfers at the walls of the enclosure. Although the mass transfer characteristics are fairly well predicted by the scale analysis, it is shown that convective heat transfer has a specific behavior in given ranges of the governing parameters.

1. INTRODUCTION

The analysis of convection heat transfer in porous media has been the subject of a very intense research activity over the past 30 years. The formulation of the macroscopic (averaged) conservation equations and the justification of the different terms usually accounted for in the classical models developed in the bibliography (Brinkman, Forchheimer) is still a relevant problem. Concerning the determination of convective heat and mass transfer in fluid saturated porous matrices, the published experimental, analytical and numerical results represent an important bibliography: a recent state of the art may be found in the book by Nield and Bejan [1].

In the field of natural convection, many studies are dealing with thermally driven flows, due to the importance of related industrial and technological applications (geothermal energy, fibrous insulating materials, some modes of assisted oil recuperation, etc.). In contrast, relatively little attention has been dedicated to the so-called double diffusive situations, where the saturating fluid consists of several constituents and where the density gradients inducing natural convection are due to coupled thermal and compositional effects.

This configuration is however fully relevant to the modeling of heat, mass and momentum transfers in materials processing involving multicomponent mixtures (alloy solidification, zone melting, etc.): a great majority of studies consider porous medium models to represent the fluid flow in the solid–liquid region, the so-called *mushy* zone. An accurate description of the phenomena in this region is of primary importance, since the physical mechanisms which rule the development of the solid phase essentially take place in this multiphase zone. Up to now, comparisons between the existing numerical simulations and the experimental results show a qualitative agreement, but important quantitative differences are still subsisting.

This work is concerned with the numerical simulation of thermosolutal natural convective flows in a porous medium. In a first stage, phase change is not accounted for, in order to focus primarily on the transport phenomena in such a medium. In the previous studies concerning thermosolutal natural convection, as it has been the case for thermal natural convection in porous media, mainly two configurations have been considered. The first situation concerns the horizontal porous layer, submitted to vertical temperature and concentration gradients. The first results on the onset of convective flows using linear stability analysis may be found in the work by Nield [2] and Taunton *et al.* [3]. More recently, this configuration has received some attention [4–12] in stability analyses, some of them taking account of heterogeneities of the porous matrix [4], of the anisotropy of the porous medium [10] or of inclined temperature and concentration gradients [11, 12]. Poulikakos [7] has studied the criterion of onset of double-diffusive convection using a Darcy–Brinkman model for describing momentum conservation in the porous medium: the results clearly show the influence of the Darcy number. Chen *et al.* [8] have also used the Brinkman and Forchheimer terms to consider nonlinear two-dimensional (2D), horizontally periodic, double-diffusive fingering convection. The stability boundaries which separate regions from different regime of convection are identified. Murray and Chen [13] have experimentally con-

NOMENCLATURE

A	aspect ratio of the enclosure, H/L
c	specific heat at constant pressure [J kg^{-1} K^{-1}]
C	dimensional mass fraction
D	mass diffusivity [m^2 s^{-1}]
Da	Darcy number, K/H^2
g	intensity of gravity [m s^{-2}]
Gr_S	solutal Grashof number based on H and on fluid properties, $= g\beta_C \Delta C H^3/\nu^2$
Gr_T	thermal Grashof number based on H and on fluid properties, $= g\beta_T \Delta T H^3/\nu^2$
$H(L)$	height (width) of the enclosure [m]
$\vec{i}(\vec{k})$	unit vector in the horizontal (vertical) direction
k	thermal conductivity [W m^{-1} K^{-1}]
K	permeability of the porous medium [m^2]
Le	Lewis number: Sc/Pr
N	buoyancy ratio: Gr_S/Gr_T
Nu	average Nusselt number (dimensionless heat flux)
P	dimensionless pressure
Pr	Prandtl number, ν/α
R_k	ratio of thermal conductivities, k_m/k_f
Ra^*	porous thermal Rayleigh number, $(Gr_T Pr Da)$
Sc	Schmidt number, ν/D
Sh	average Sherwood number (dimensionless mass flux)
T	dimensional temperature [K]
$u(w)$	horizontal (vert.) dimensionless component of velocity
$\vec{V}$	dimensionless velocity
$x(z)$	dimensionless coordinates, x^*/H (z^*/H).

Greek symbols

α	thermal diffusivity [m^2 s^{-1}]
β_T	coefficient of volumetric expansion with temperature [K^{-1}]
β_S	coefficient of volumetric expansion with mass fraction
ΔC	concentration difference between plates, $C_1 - C_2$
ΔT	temperature difference between plates, $T_1 - T_2$
Λ	viscosity ratio μ_{eff}/μ
ε	porosity of the porous medium
μ	dynamic viscosity of the fluid [kg m^{-1} s^{-1}]
μ_{eff}	viscosity in the Brinkman model
ν	kinematic viscosity [m^2 s^{-1}]
Φ	dimensionless concentration: $(C-(C_2+C_1)/2)/\Delta C$
ρ	fluid density [kg m^{-3}]
σ	ratio of specific heats, $(\rho c)_m/(\rho c)_f$
Θ	dimensionless temperature: $(T-(T_2+T_1)/2)/\Delta T$.

Subscripts

0	reference (average value)
1	hot side
2	cold side
f	fluid
H	based on H
m	fluid-saturated porous medium
S	solutal
T	thermal.

Superscript

(*)	indicates dimensional quantities, except in Ra^*.

firmed within 10% the critical thermal Rayleigh number obtained by Nield [2]. Trevisan and Bejan [14] have determined analytically the mass transfer due to thermally driven flows at high Rayleigh numbers. Their numerical results and a scaling analysis allow us to conclude that mass transfer depends on different scaling laws, depending on the Lewis number. The transition between the Darcy and the Forchheimer regimes has also been documented. A recent study by Rosenberg and Spera [15] deals with the influence of the Rayleigh, Lewis and buoyancy numbers on the heat and mass transfer in steady and unsteady states, considering several types of initial conditions. Lately, Mamou *et al.* [16] compare an approximate analytical solution to numerical simulations for a shallow cavity with uniform heat and mass fluxes specified at the horizontal walls. The critical Rayleigh number is obtained as a function of the Lewis and buoyancy numbers.

In the vertical configuration (horizontal temperature and concentration gradients), the first studies are concerned with the destabilization of compositionally stratified layers [17–20]. Raptis *et al.* [21] present an analytical solution for the semi-infinite cavity. A few authors have studied the boundary layer flow [22–24], showing various regimes according to the value of the Lewis number and of the ratio of buoyancy forces. Trevisan and Bejan [25] have considered a square cavity submitted to horizontal temperature and concentration gradients: a numerical study based on the Darcy model is compared to a scaling analysis, over a range of relatively moderate values of the parameters ($0.1 \leqslant Le \leqslant 10$, $-5 \leqslant N \leqslant 3$ and $Ra^* = 200$ for $N \neq 0$). Recently, transient double

diffusive natural convection in a square enclosure has been investigated numerically [26, 27], for moderate buoyancy ratio and Lewis number. Other boundary conditions have been considered in this geometry [28–31].

In the vertical configuration, all the above studies describe the momentum conservation in the porous medium using the Darcy model. Because our main objective is to study double diffusive natural convection in the context of solidification, where permeability and porosity are not constant in space and time, the Darcy–Brinkman formulation is adopted in the present study. We first give a description of the problem, then the governing equations are recalled and the numerical method briefly outlined. The section presenting the numerical results is divided into two parts: one is dedicated to the analysis of mass transfer and the other to heat transfer. The influence of the main dimensionless parameters is considered, and special attention is given to the role of the Brinkman term in the Darcy model.

2. PROBLEM DEFINITION

The present work refers to the study of natural convective flows in a porous cavity (height H, width L: aspect ratio $A = H/L$), saturated by a binary fluid (such as aqueous solutions, as in numerous experimental studies related to solidification processes). Horizontal temperature and concentration differences are specified between the vertical walls (T_1 and C_1 at the left wall, T_2 and C_2 at the right wall), and zero mass and heat fluxes are imposed at the horizontal walls. All the boundaries are impermeable. The binary fluid is assumed to be Newtonian and to satisfy the Boussinesq approximation; the flow is incompressible, laminar, 2D and in the steady state. On the other hand, the porous medium is supposed to be isotropic, homogeneous and in thermodynamical equilibrium with the fluid. The Soret and Dufour effects are assumed to be negligible. The density variations upon temperature and concentration are described by the state equation:

$$\rho = \rho_0[1-\beta_T(T-T_0)-\beta_C(C-C_0)] \quad (1)$$

where:

$$\beta_T = -\frac{1}{\rho}\left[\frac{\partial\rho}{\partial T}\right]_C \quad \text{and} \quad \beta_C = -\frac{1}{\rho}\left[\frac{\partial\rho}{\partial C}\right]_T. \quad (2)$$

Using the following dimensionless variables: $x = x^*/H$, $z = z^*/H$, $V = \vec{V}^*H/v$, $t = t^*v/H^2$, $P = P^*H^2/\rho v^2$, $\Theta = (T-T_0)/\Delta T$ and $\Phi = (C-C_0)/\Delta C$ (where H is the cavity height and v the kinematic viscosity of the fluid), the macroscopic conservation equations describing transport phenomena in the cavity are:

$$\vec{\nabla}\cdot\vec{V} = 0 \quad (3)$$

$$\frac{1}{\varepsilon}\frac{\partial\vec{V}}{\partial t} + \frac{1}{\varepsilon^2}(\vec{V}\cdot\vec{\nabla})\vec{V} = -\vec{\nabla}P + (Gr_T\Theta + Gr_S\Phi)\vec{k} - \frac{1}{Da}\vec{V} + \Lambda\nabla^2\vec{V} \quad (4)$$

$$\sigma\frac{\partial\Theta}{\partial t} + \vec{V}\cdot\vec{\nabla}\Theta = \frac{1}{Pr}R_k\nabla^2\Theta \quad (5)$$

$$\varepsilon\frac{\partial\Phi}{\partial t} + \vec{V}\cdot\vec{\nabla}\Phi = \frac{1}{Sc}\nabla^2\Phi \quad (6)$$

where $Gr_T = (g\beta_T\Delta TH^3)/v^2$ and $Gr_S = (g\beta_C\Delta CH^3)/v^2$ are the thermal and the solutal Grashof numbers, respectively. $Da = K/H^2$ is the Darcy number, $Pr = v/\alpha$ the Prandtl number, $Sc = v/D$ the Schmidt number and the ratio $Le = Sc/Pr$ the Lewis number (see nomenclature). Equation (4) stands for the Darcy–Brinkman momentum equation where, according to Lauriat and Prasad [32] the Forchheimer inertia term has been neglected since in all the computations performed in this study, the Reynolds number defined by:

$$Re = \frac{\rho v K^{1/2}}{\mu} \quad (7)$$

is less than unity. The source term in the momentum equation is written in terms of the fluid Grashof numbers, but the porous thermal Rayleigh number Ra^*, defined as: $Ra^* = Da\cdot Pr\cdot Gr_T$ will be used in the analysis of the results.

Λ is the ratio of the viscosity in the Brinkman term to the fluid viscosity. Lundgren [33] has computed values for the effective viscosity in several configurations of porous media. He found that the ratio Λ was a function of the porosity. In a very recent paper, Gilver and Altobelli [34] determine experimentally the effective viscosity by using a NMR technique. The effective viscosity appears to be insensitive to flow rate when the Reynolds number is less than 20. σ and R_k are the ratios of the thermophysical properties of the porous medium and of the fluid, for the specific heat $\sigma = (\rho c)_m/(\rho c)_f$ and for the thermal conductivity $R_k = k_m/k_f$, respectively. The average heat and mass fluxes at the walls are given in dimensionless terms by the Nusselt and the Sherwood numbers:

$$Nu = \int_0^1 \left[\frac{\partial\Theta}{\partial x}\right]_{x=0} dz \quad Sh = \int_0^1 \left[\frac{\partial\Phi}{\partial x}\right]_{x=0} dz. \quad (8)$$

3. NUMERICAL METHOD

The finite volume method [35] is used to discretize the governing equations (3)–(6). As a consequence of the very thin solutal boundary layers to be expected in such problems, irregular grids are used: the size and distribution of the nodes are depending on the range of parameters, and it has been checked that at least five nodes are present in the thinnest boundary layer. In the square cavity ($A = 1$), the simulations

Table 1. Average Nusselt number for $N = 0$ at $A = 1$ (Darcy model: $Da \leqslant 10^{-7}$)†

Ra_L^*	100	200	500	1000
Present work	2.08	3.04	4.94	7.05
Lauriat *et al.* [32]	2.08	3.03	4.92	7.02
Prasad *et al.* [37]	2.06	3.01	4.96	7.25

† The Rayleigh and Nusselt numbers are built on L.

are generally performed using a 64×64 sinusoïdal grid for moderate solutal Rayleigh numbers (see section 4) and a 145×95 sinusoïdal grid at high solutal Rayleigh numbers. The discretization technique is well-known and a detailed description is not needed: only the main characteristics are presented hereafter. The integral equations are discretized using the hybrid scheme of Patankar and Spalding [35], and the linear systems derived from the conservation equations are solved using a line by line procedure, allowing for the use of a fast tridiagonal matrix algorithm (TDMA). As the momentum equation is formulated in terms of the primitive variables (velocity and pressure) the iterative procedure includes a pressure correction calculation method to solve the pressure–velocity coupling. The code uses the classical SIMPLE technique [35] for the pressure and velocity correction. The convergence criterion is based on the average residue of the continuity equation on the whole domain and convergence is reached when this residue is less than 10^{-6}. The numerical results presented in this paper have been performed on a Cray-C98 vectorial computer. An excellent level of vectorization of the code (95% of the execution in the vectorial mode) has been obtained by vectorizing the central TDMA, where most of the CPU time is spent.

The validation of the numerical code has been performed over a large range of parameters for purely thermal natural convection in porous media: some comparison results are presented hereafter, for the Darcy model (Table 1), and for the extended Brinkman formulation (Table 2). It may be seen from the results that the agreement with reference solutions available in the bibliography [32, 36] is excellent for both regimes.

Results concerning mass transfer due to purely thermal natural convection ($N = 0$) are presented in Table 3 for $Le = 10$. In this configuration, the solutal buoyancy force is not present, but mass transfer is induced by the thermally driven flow. As the Lewis number is larger than 1, the mass transfer is higher than the corresponding heat transfer. To our knowledge, the only available results in this configuration have been proposed by Trevisan and Bejan [25], and the calculated values of the Nusselt and Sherwood numbers are compared in Table 3. The discrepancy between the results is particularly significant at the higher values of the Rayleigh number ($Ra^* = 400$). As a consequence of the good validation of our code in this range of parameters for the pure thermal case (which is still the case at $N = 0$), it seems that the results proposed in ref. [25] somewhat overestimate the Nusselt and Sherwood numbers.

More results concerning the Darcy model in the $N = 0$ situation on a range of Le and Ra^* values are displayed in Table 4. As expected, the Nusselt number does not depend on the Lewis number for a given Ra^*, since the flow is totally driven by the thermal buoyancy force. On the other hand, the Sherwood number is clearly seen to increase with increasing Le or Ra^* numbers. The mass transfer results are plotted on Fig. 1 as a function of $Ra^* \times Le$. Our results are in close agreement with the scaling law derived in [25], which leads to:

$$Sh \sim (Ra^* Le)^{1/2} \tag{9}$$

since the power law deduced from the computed values of the Sherwood number gives:

$$Sh = 0.40(Ra^* Le)^{0.51}. \tag{10}$$

Finally, the numerical simulations of thermosolutal natural convection at high values of the Darcy number ($Da \sim 1$) give the same results as those previously obtained in fluids [37].

Table 2. Average Nusselt number for $N = 0$ at $A = 5$ (Darcy–Brinkman model)

Da		10^{-7}	10^{-5}	10^{-4}	10^{-3}	10^{-2}
$Ra^* = 500$	Present work	10.39	10.34	10.00	9.13	7.29
	Lauriat *et al.* [32]	10.40	10.25	9.95	9.15	7.25
$Ra^* = 1000$	Present work	15.19	14.99	14.28	12.55	9.44
	Lauriat *et al.* [32]	15.15	14.90	14.30	12.60	9.45

Table 3. Average Nusselt and Sherwood numbers ($N = 0$, $Le = 10$, $A = 1$)

Ra^*		100	200	400	1000	2000
Nu	Present work	3.11	4.96	7.77	13.47	19.90
	Trevisan and Bejan [25]	3.27	5.61	9.69	—	—
Sh	Present work	13.25	19.86	28.41	48.32	69.29
	Trevisan and Bejan [25]	15.61	23.23	30.73	—	—

Table 4. Average Nusselt and Sherwood numbers (Darcy model: $N = 0$, $A = 1$)

Ra^*	Le	Nu	Sh	Ra^*	Le	Nu	Sh
	1	1.98	1.98		1	8.93	8.93
	10	1.98	8.79		10	8.93	33.27
50	—	—	—	500	20	8.93	46.77
	—	—	—		50	8.93	72.17
	100	1.98	27.97		100	8.93	99.23
	1	3.11	3.11		1	13.47	13.47
	10	3.11	13.25		10	13.47	48.32
100	20	3.11	18.89	1000	20	13.47	67.45
	50	3.11	29.72		50	13.47	103.10
	100	3.11	41.53		100	13.47	140.65
	1	4.96	4.96		1	19.90	19.90
	10	4.96	19.86		10	19.90	69.29
200	20	4.96	28.17	2000	20	19.90	96.03
	50	4.96	44.00		50	19.90	145.32
	100	4.96	61.09		100	19.90	196.62

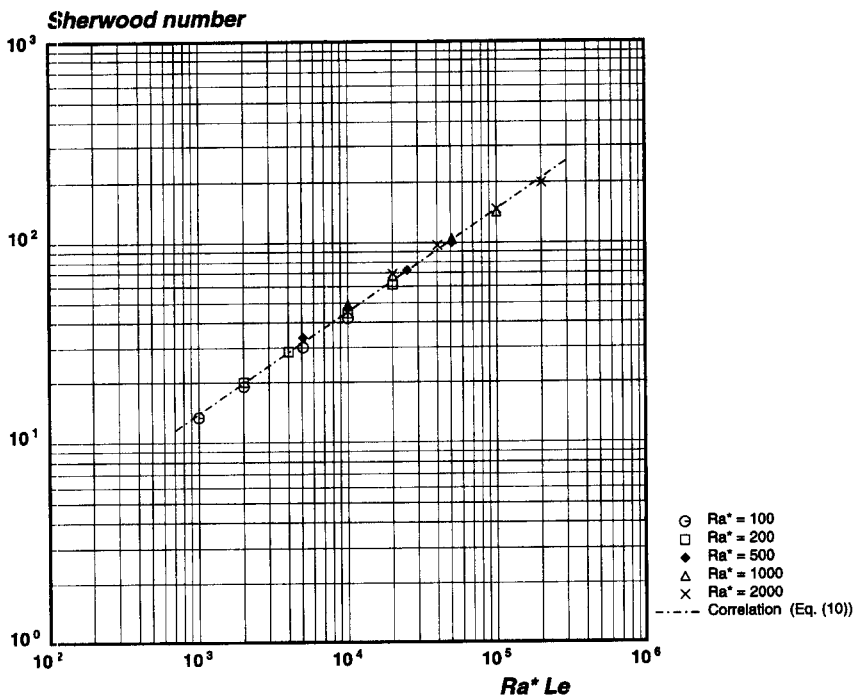

Fig. 1. Mass transfer by thermal natural convection (Darcy model; $A = 1$; $N = 0$).

4. NUMERICAL RESULTS

The numerical code described above has been used to perform a number of simulations concerning double diffusive natural convection in homogeneous and isotropic porous media. The range of parameters that has been examined in this study concerns the $N > 0$ domain (cooperating buoyancy forces). The value of N has been generally taken between 0 and 50 for different values of the thermal Rayleigh number Ra^*, ranging from 100 to 1000. All the simulations are performed in the range $Le > 1$: relatively high values of Le have been used, between 10 and 300. The other parameters have been kept constant: the aspect ratio of the enclosure ($A = 1$), the Prandtl number of fluid ($Pr = 10$), as well as the porous medium properties ($\Lambda = 1$, $\sigma = 1$ and $R_k = 1$). The Brinkman extended Darcy model has been used through the study: in a first step, the Darcy equation is used (corresponding to a Darcy number $Da \approx 10^{-7}$), then the influence of the Brinkman term due to increasing viscous forces ($Da = 10^{-5}$–10^{-3}) is analyzed. Due to the large number of parameters, and in order to separate the influence on heat transfer and on mass transfer, the results are first presented in terms of the Sherwood number, and then the heat transfer characteristics are analyzed.

4.1. *Mass transfer*

In this section, the influence of the governing parameters on mass transfer (the average Sherwood number at the vertical walls) is analyzed in the range $N > 1$

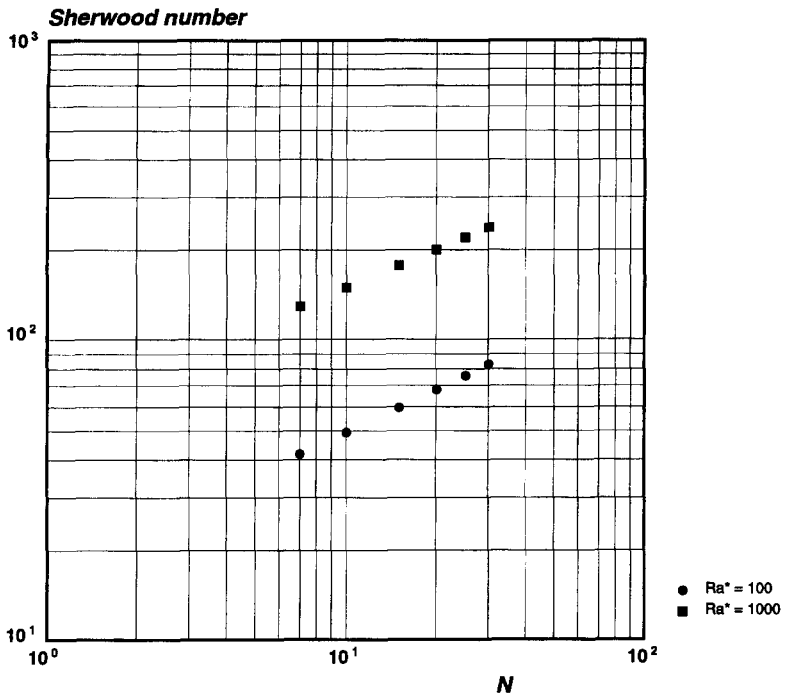

Fig. 2. Sherwood number as a function of the buoyancy ratio ($Le = 10$; $Ra^* = 100$ and 1000, $A = 1$).

and $Le > 1$. Since the solutal buoyancy force is dominating over the thermal one, and the thermal diffusivity is larger than the molecular diffusivity, this configuration belongs to the 'mass transfer driven' flow identified in the analysis by Trevisan and Bejan [25]: assuming the boundary layer approximation, these authors show that the relevant parameter for scaling the solutal boundary layer thickness in the Darcy regime, and thus the mass transfer, is the modified solutal Rayleigh number (Ra^*LeN). The scale analysis [25] leads to:

$$Sh \approx (Ra^*LeN)^{1/2} \tag{11}$$

a correlation which is strictly analogous to the Nu–Ra^* correlation in thermal convection. This section is dedicated to the analysis of the numerical results in this situation, and of the influence of the viscous term in the Darcy–Brinkman model.

4.1.1. *Darcy model* ($\mathrm{Da} \leqslant 10^{-7}$). In the simulations presented hereafter, we first analyze the influence of the buoyancy number, N ranging from 2 to 30. At $Le = 10$, the results displayed in Fig. 2 have been obtained for two values of the modified thermal Rayleigh number: $Ra^* = 100$ and $Ra^* = 1000$. As expected, it appears on the graph that the Sherwood number increases with N and Ra^*: this confirms the fact that the global buoyancy term in the momentum equation, $Gr_T(\Theta + N\Phi)$, increases with Gr_T and N, enhancing the flow velocity and the overall transfer.

At $Ra^* = 100$ (Fig. 3), results are obtained for different values of the Lewis number, $Le = 30$ and $Le = 300$. The mass transfer is seen to increase with the Lewis number for given N and Ra^*. Indeed, the Lewis number is increased through the Schmidt number (Pr is fixed), which directly reduces the solutal boundary layer thickness, and leads to a higher Sherwood number. The results displayed in Figs. 2 and 3 also show the power law dependence of the Sherwood number with N.

Using these first observations, the numerical results obtained on the whole range of parameters given above are displayed in Fig. 4 as a function of the solutal Rayleigh number (Ra^*LeN): it is clear that the relevance of this parameter to correlate the mass transfer results and the power-law dependence are confirmed by the computations. A regression of the results—expecting the lower values of N where the solutal buoyancy force is not fully dominating the flow—leads to the following correlation:

$$Sh = 0.75(Ra^*LeN)^{0.46} \tag{12}$$

where the exponent is in fairly good agreement with the value 1/2 assessed by the scale analysis.

As a matter of fact, the lack of continuity between the scaling laws given by correlation (10) when $N = 0$ and equation (12) when $N \gg 1$ suggests to propose a more general correlation, which could be used on the whole N range. Considering the expression of the source term in the Darcy equation: $Gr_T(\Theta + N\Phi)$, we may retain $Gr_T(N+1)$ as an order of magnitude of the driving term, and propose a correlation as a function of $Ra^*Le(N+1)$, which would satisfy both limits (the same proposal has been made in [25] to account for the singularity at $N = -1$). The results obtained on the whole range of parameters (including $N = 0$) con-

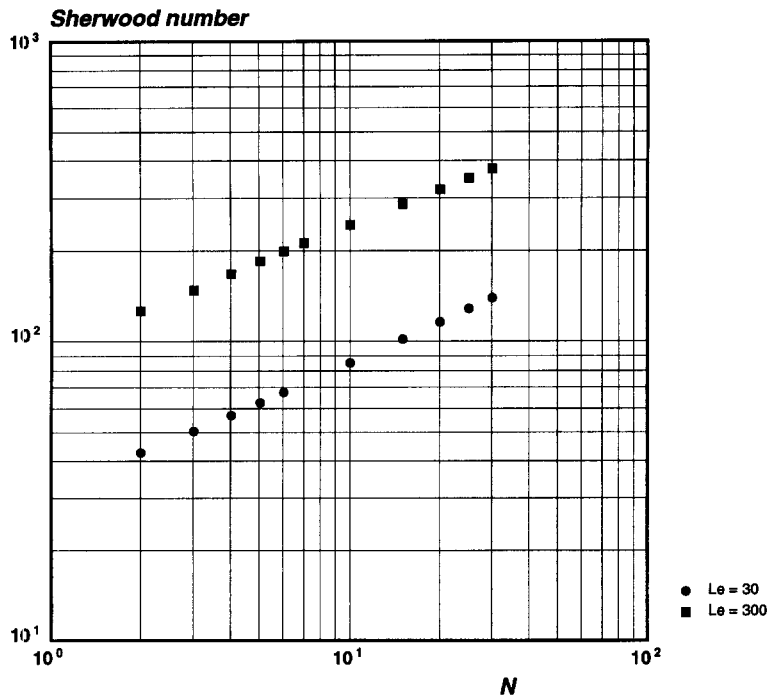

Fig. 3. Sherwood number as a function of the buoyancy ratio ($Ra^* = 100$; $Le = 30$ and 300, $A = 1$).

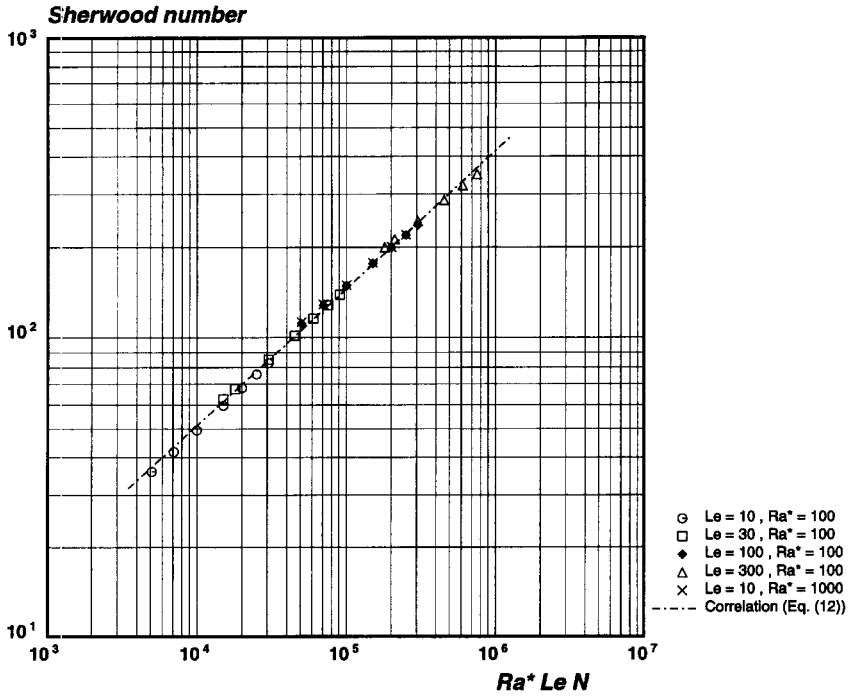

Fig. 4. Sherwood number vs the solutal Rayleigh number (Darcy model; $A = 1$).

sidered in this parametric study are plotted in Fig. 5, and the following correlation is obtained:

$$Sh = 0.54(Ra^* Le(N+1))^{0.48}. \quad (13)$$

Again, the exponent is clearly in the range expected from the scaling laws.

4.1.2. *Darcy–Brinkman model.* In this section, the influence of the Darcy number is investigated. For given values of Le and Ra^*, and N varying from 2 to 30, increasing values of Da are chosen, from 10^{-7} (the Darcy regime) to 10^{-3}. The results for $Ra^* = 100$ at $Le = 100$ are represented in Fig. 6.

In the field of purely thermal natural convection, it is now well-known (see for instance [32]) that the heat

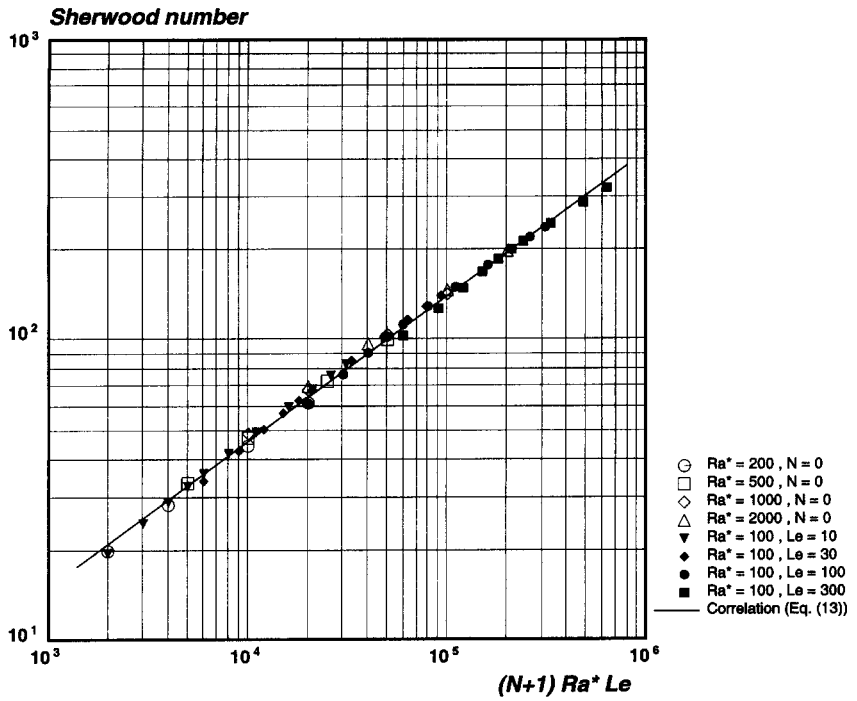

Fig. 5. Mass transfer in the Darcy regime as a function of the dimensionless group $(N+1)\ Ra^*\ Le$.

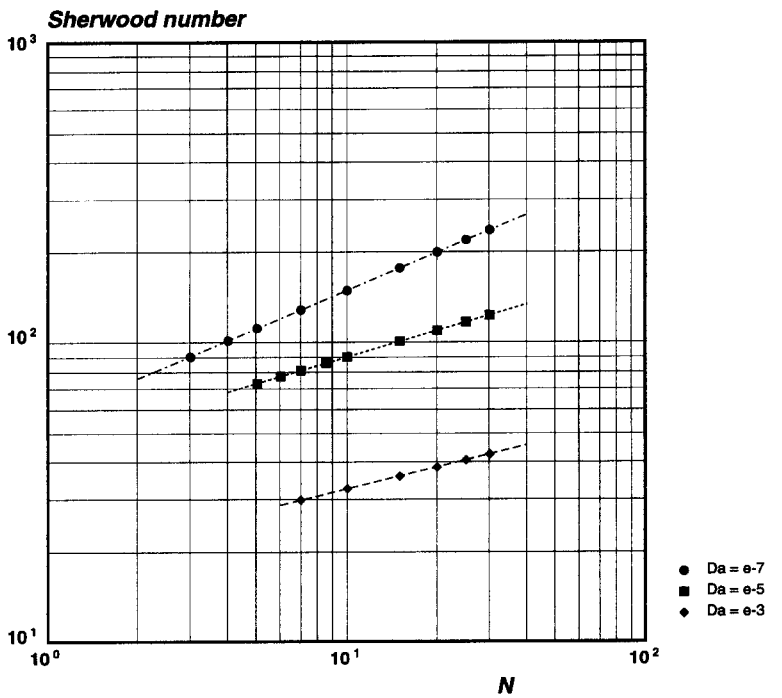

Fig. 6. Variation of mass transfer with N: influence of the Darcy number ($Ra^* = 100$; $Le = 100$; $A = 1$).

transfer decreases with increasing Darcy numbers, and that the rate of decrease is more significant at higher Rayleigh numbers. A similar behavior may be expected for mass transfer in mass driven thermosolutal convection. Indeed, increasing the Brinkman term implies that the balance between the Darcy term and the buoyancy force in the boundary layer is progressively replaced by a viscous force vs buoyancy term balance at high Darcy numbers, reducing the velocity on this scale [1]. An interesting feature of these results is that the linearity of the $\log(Sh)$ vs $\log(N)$ graphs is verified for all the situations represented on the figure, and that the slope depends on the Darcy number.

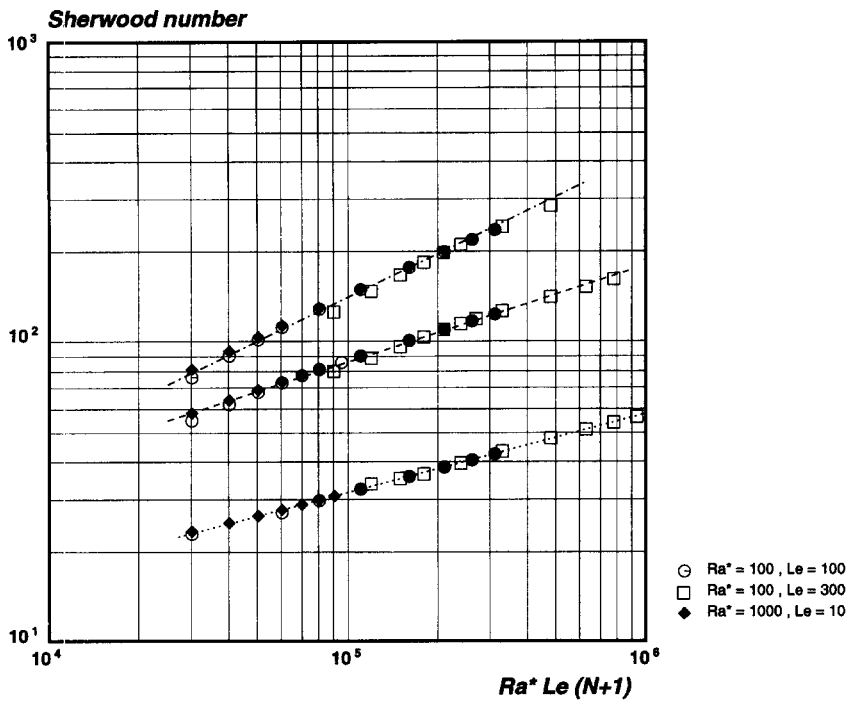

Fig. 7. Variation of mass transfer with the dimensionless group $(N+1)\ Ra^*\ Le$. Influence of the Darcy number.

If we refer to the results presented in the previous section, the correlation between the Sherwood number and the solutal Rayleigh number when Da is increased is expected to shift from a porous medium behavior (that is, a $[Ra^*Le(N+1)]^{1/2}$ law) to a fluid behavior (a 1/4 power law). Figure 7 gives a representation of the results obtained for ($Ra^* = 100$ at $Le = 100$), ($Ra^* = 1000$ at $Le = 10$) and ($Ra^* = 100$ at $Le = 300$). The influence of Da on the power law is clearly seen on the plot: the slope varies from 0.48 at $Da = 10^{-7}$ to 0.32 at $Da = 10^{-5}$ and 0.26 at $Da = 10^{-3}$. A correlation giving explicitly the influence of the Darcy number on both the exponent and the cofactor has still to be found, and more computations are necessary to investigate the influence of Da for fixed values of Gr_T on a wider range of Darcy numbers.

The effect of the viscous forces accounted for in the Brinkman term on the flow velocity is illustrated in Fig. 8. The different fields corresponding to $N = 10$, $Ra^* = 100$ and $Le = 10$ are represented in Fig. 8(a) for $Da = 10^{-7}$ and Fig. 8(b) at $Da = 10^{-3}$. The streamlines show that the dynamic boundary layers are thicker for the higher value of Da, and consequently the concentration gradients at the walls are smaller when the Brinkman term becomes significant. The concentration field present the classical stratified structure of the natural convective flows in enclosures, but the isotherms show a different behavior of the temperature field: for studying the heat transfer, it is clear that the boundary layer analysis is not adapted. It is interesting to note that this feature is similar to the observations made for thermosolutal natural convection in fluids for a certain range of buoyancy ratio and thermal Rayleigh numbers.

4.2. *Heat transfer*

As far as heat transfer is concerned, the influence of the governing parameters on the Nusselt number has been analyzed by Trevisan and Bejan [25] who proposed scaling laws in the range of moderate Lewis numbers and mass transfer driven flows ($N \gg 1$). The scale analysis leading to equation (11) for mass transfer yields:

$$Nu \approx \left(Ra^* \frac{N}{Le}\right)^{1/2}. \tag{14}$$

The overall increase of the average heat transfer due to Ra^* or N is expected, because both parameters directly contribute to enhance the buoyancy term in the momentum equation, and thus the convective heat transfer. The Nusselt number decrease with Le is due to the fact that:

$$\delta_T/\delta_C \approx Le. \tag{15}$$

Then, as the solutal boundary layer thickness is known to decrease as $Le^{-1/2}$, the thermal boundary layer thickness is a function of $Le^{1/2}$ and the Nusselt number decreases with Le.

Let us note that in the particular situation where $Le = 1$, the Nusselt and Sherwood numbers are identical, and equations (11) and (14) lead to the same expression.

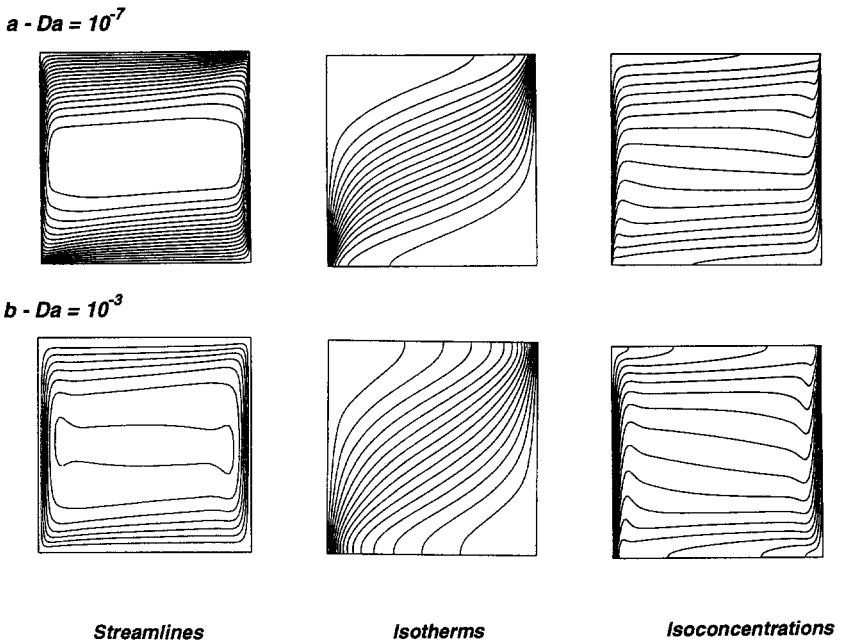

Fig. 8. Streamlines, isotherms and isoconcentration lines ($Ra^* = 100$; $Le = 10$; $N = 10$; $A = 1$): (a) $Da = 10^{-7}$; (b) $Da = 10^{-3}$ ($\Delta\psi = 0.046$; $\Delta\theta = 1/17$; $\Delta\phi = 1/17$).

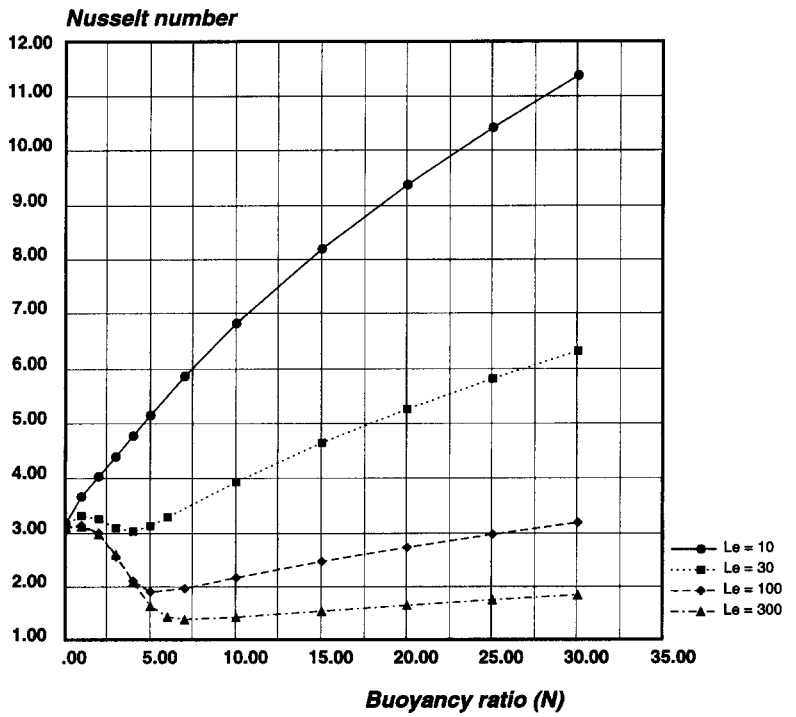

Fig. 9. Variation of the Nusselt number with the buoyancy number N: influence of the Lewis number ($Ra^* = 100$; $Da = 10^{-7}$; $A = 1$).

4.2.1. *Influence of* N *in the low* Le *range*. Figure 9 displays the Nusselt number as a function of N for different values of Le ranging from 10 to 300, at $Ra^* = 100$ and $Da = 10^{-7}$. If one considers the plot corresponding to the $Le = 10$ results, it is clear on the graph that the preceding analysis applies. The set of results obtained at $Le = 10$ in the Darcy regime, for $Ra^* = 100$ and 1000, and N ranging from 5 to 30, leads to the following correlation:

$$Nu = 0.76\left(Ra^* \frac{N}{Le}\right)^{0.48} \tag{16}$$

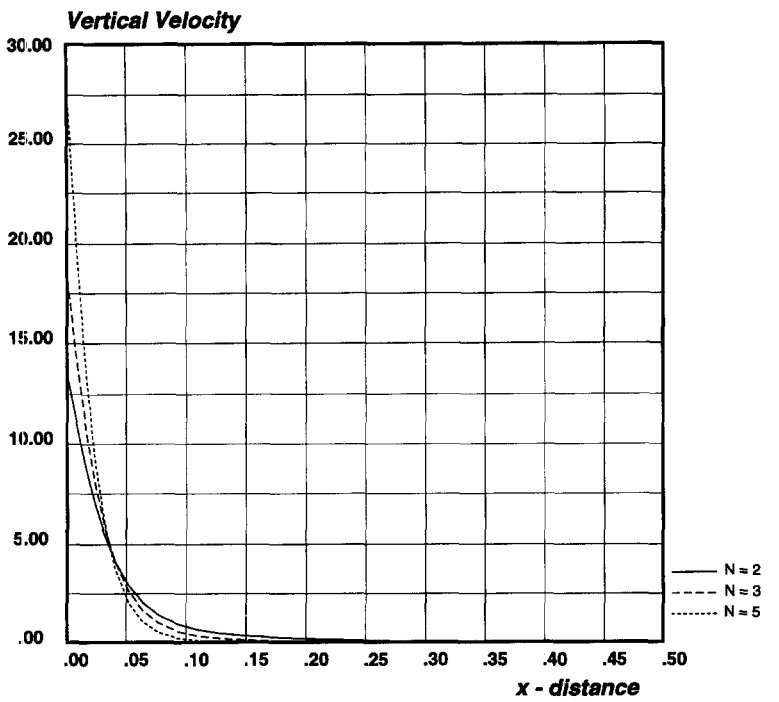

Fig. 10. Vertical velocity profiles in the horizontal midplane at $Le = 10$ ($Ra^* = 100$; $Da = 10^{-7}$; $A = 1$).

which confirms the scale analysis, and is in excellent agreement with equation (12) for $Le = 1$.

The influence of N on the average heat transfer means that the convective transport of heat increases with N. This is well illustrated by the vertical velocity profiles in the horizontal midplane displayed in Fig. 10 for $N = 2$, 3 and 5 ($Ra^* = 100$, $Da = 10^{-7}$, $Le = 10$). Those profiles clearly show that the velocity maximum continuously increases, and that the thickness of the corresponding boundary layer decreases with N: stronger convection, due to a larger buoyancy ratio, results in enhanced heat transfer.

However this description is shown to hold only in a range of moderate Lewis numbers. The results displayed in Fig. 9 for different values of Le ranging from 30 to 300 ($Ra^* = 100$ and $Da = 10^{-7}$) show that, although the decrease of the Nusselt number with increasing Le is verified by the calculations, the increase of the overall buoyancy term through N does not necessarily enhance the heat transfer in the cavity. This behavior is in contradiction with the scaling law expressed by equation (14), and it requires a more detailed analysis.

4.2.2. *Influence of* N *at* Le $\gg$ 1. Let us consider the curve in Fig. 9 corresponding to $Le = 100$: the Nusselt number results displayed in the Darcy regime clearly show that Nu is first relatively insensitive to N for the very low values of the buoyancy ratio, then Nu *decreases*, undergoes a minimum (here for $N \approx 5$–6), and again slightly increases at higher values of N. The same behavior may be qualitatively observed for $Le = 30$ or $Le = 300$. As mentioned earlier when examining the results of Fig. 9, the influence of the Lewis number is that the overall Nusselt number decreases with Le. Furthermore, the N value corresponding to Nu_{min} gets larger when the Lewis number is increased.

At $Le = 30$ however, the initial decrease is preceded by a first maximum, showing that this value of the Lewis number is intermediate between the present behavior, characterizing the 'high Lewis number range' and the 'low Lewis number behavior' described in the previous section.

In order to give an interpretation of the behavior at a high Lewis number, the vertical velocity profile in the horizontal midplane is represented in Fig. 11 for different values of N in the vicinity of the minimum Nusselt number ($Ra^* = 100$, $Le = 100$, $Da = 10^{-7}$). For $N = 2$, the reduced velocity profile is represented in Fig. 12, together with the temperature and concentration distributions in the $z = 0.5$ plane. Two distinct zones are clearly identified on the velocity profiles, which are enlarged on the figure (Fig. 11):

(1) a thin boundary layer close to the wall and
(2) a velocity maximum in the core of the flow.

In the range $x < 0.05$, it is possible to observe the direct influence of N on the vertical velocity scale. The boundary layer is mainly due to the solutal buoyancy term at the scale of the solutal boundary layer δ_C, which is of order 10^{-2} in the present situation (Fig. 12). The classical scaling laws apply and the velocity scale continuously grows with increasing N.

Let us note that, although these results correspond

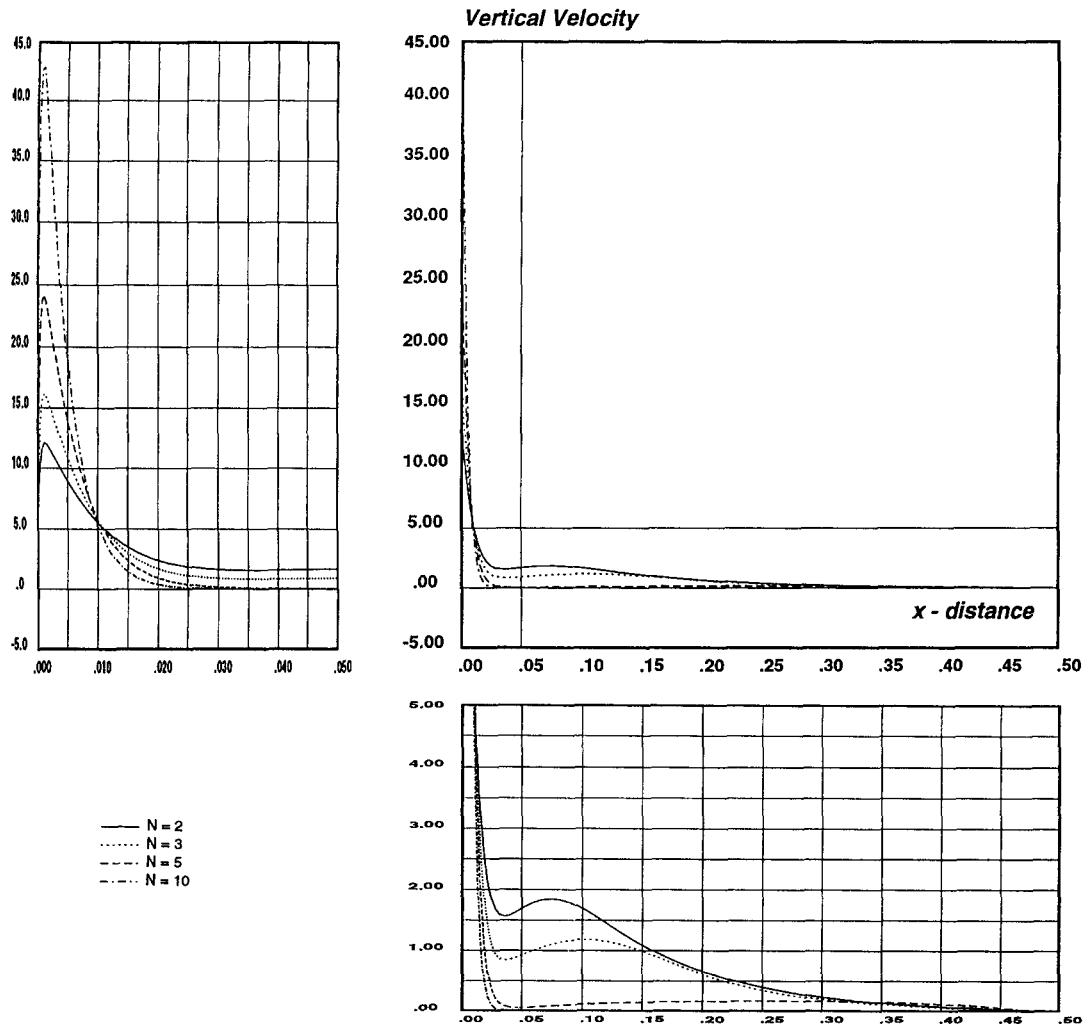

Fig. 11. Vertical velocity profiles in the horizontal midplane at $Le = 100$ ($Ra^* = 100$; $Da = 10^{-7}$; $A = 1$).

to the Darcy regime, the Darcy–Brinkman extended formulation has been used in the computations, and the no-slip boundary condition is retained at the wall.

If we now refer to the inner part of the enclosure ($0.05 < x < 0.5$), it may be seen (Fig. 12) that the local maximum is due to the thermal buoyancy term, the influence of which is felt on a much larger x-scale; typically one fourth of the total width. This effect is extremely sensitive to the N value, and, as expected, this contribution decreases when the solutal buoyancy term becomes progressively dominant through the increase of N.

So, the decrease of the Nusselt number at low values of N is due to the fact that the initial damping of the velocity in the core (due to the thermal effect) is stronger than the enhancement of the velocity close to the wall (due to the solutal one). Then, when the contribution of the thermal buoyancy term on the velocity field becomes negligible (in this case, around $N = 5$), the heat transfer slightly increases with N due to the velocity increase on the δ_C scale. Such a behavior characterizes the intermediate region between heat transfer dominated and mass transfer dominated thermosolutal convection. It appears that the plain boundary layer approximation is not valid in this range, where no complete scale analysis is available.

This local interpretation is confirmed by the observations of the flow, temperature and concentration fields plotted in Fig. 13 for different values of N ($Ra^* = 100$, $Le = 100$, $Da = 10^{-7}$). It may be seen on the streamlines that increasing N significantly modifies the flow structure: at low N, the whole enclosure is affected by the flow, and a boundary layer regime progressively appears with larger N. This modification of the flow structure has a direct visible consequence on the concentration field, which progressively builds up a vertical stratification. Although this transition towards a solutally dominated regime corresponds to a heat transfer minimum, the consequence on the temperature field is barely visible: the minimum is seen however to coincide with the end of a temperature stratification.

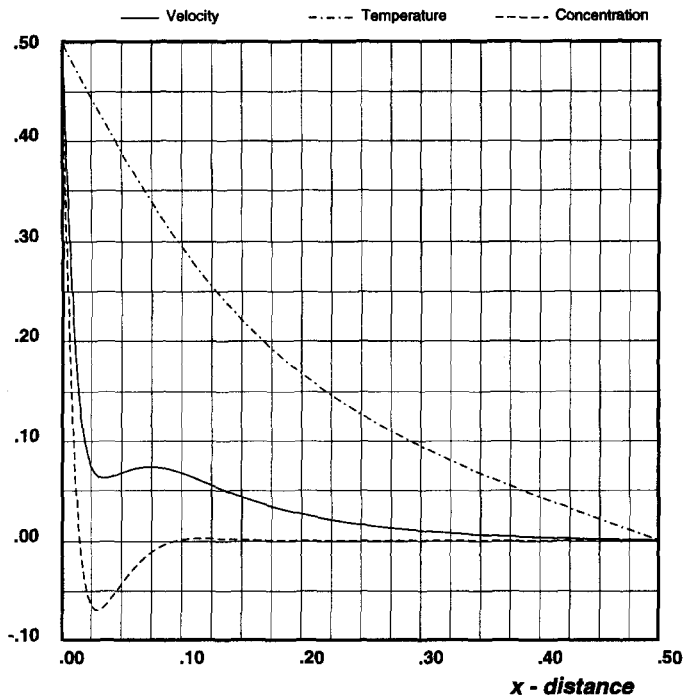

Fig. 12. Vertical velocity, temperature and concentration profiles in the horizontal midplane ($Ra^* = 100$; $Da = 10^{-7}$; $A = 1$; $N = 2$; $Le = 100$).

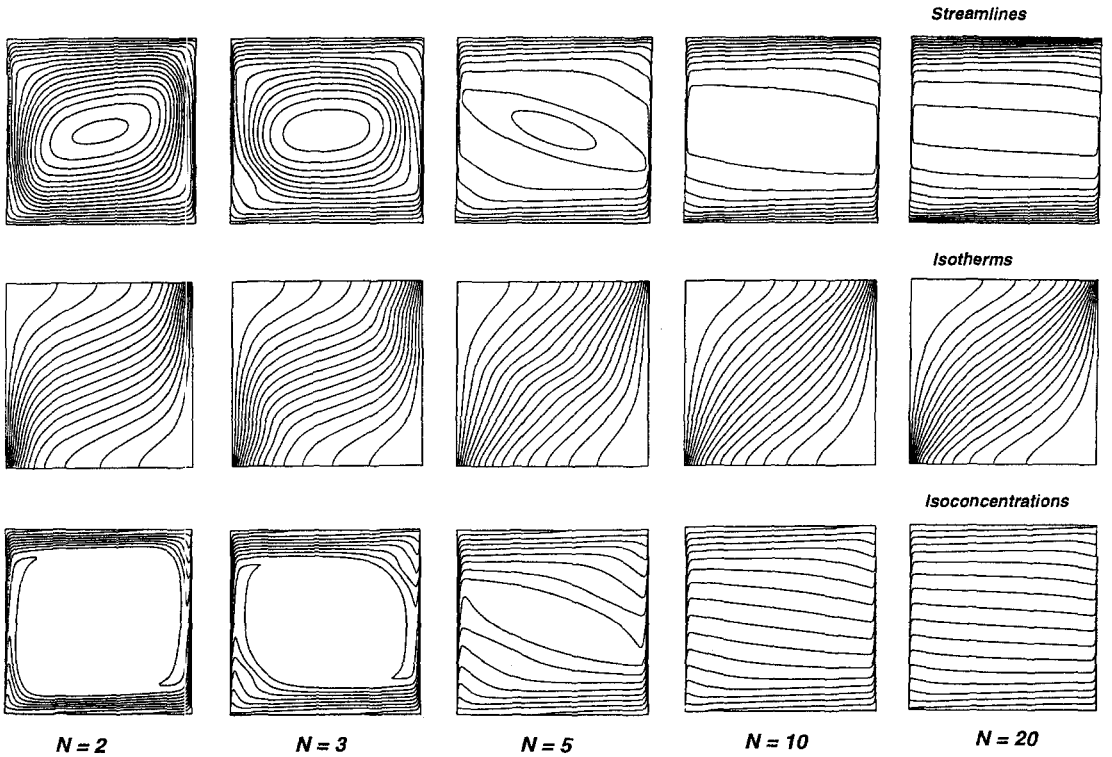

Fig. 13. Streamlines, isotherms and isoconcentration lines, Darcy regime ($Ra^* = 100$; $Da = 10^{-7}$; $Le = 100$; $A = 1$). ($\Delta\psi = 0.026$; $\Delta\theta = 1/17$; $\Delta\phi = 1/17$).

4.2.3. *Influence of the Darcy number.* The numerical results described in the previous section have been obtained in the Darcy regime, and we now analyze the results obtained with the Darcy–Brinkman model. Figure 14 displays the Nusselt number variation with N for a given Rayleigh number ($Ra^* = 100$) at

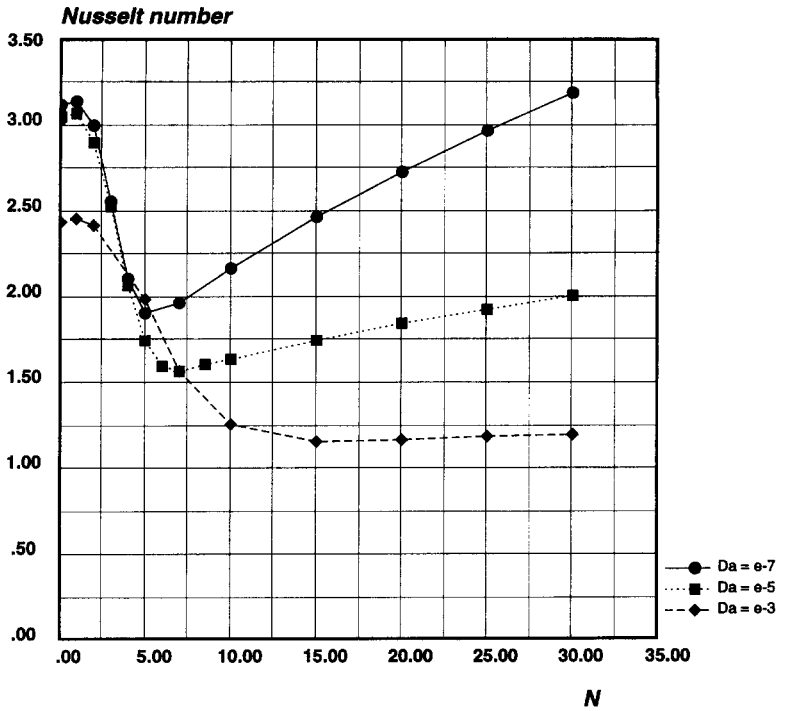

Fig. 14. Variation of the Nusselt number with the buoyancy number N: influence of the Darcy number ($Ra^* = 100$; $Le = 100$; $A = 1$).

$Le = 100$ and different values of the Darcy number, ranging from the simple Darcy model ($Da = 10^{-7}$) to the Brinkman dominated regime ($Da = 10^{-3}$). It may be seen on the figure that the Nusselt number dependence on N is extremely sensitive to the Darcy number, that is to the influence of the viscous terms in the momentum equation. While the decrease of Nu with moderate values of N is present for all Da values, it may be observed that there is no local Nu minimum for the higher values of Da. The existence of this minimum seems to be characteristic of the Darcy regime (low Da values), and the presence of a dominating Brinkman term leads to a behavior which has been observed for thermosolutal natural convection in fluids. At high Lewis numbers [35], it has been shown that the Nusselt number tends to a pure conduction limit ($Nu \approx 1$) when the buoyancy ratio is increased. In fluids, this is generally associated to the formation of a multicellular regime which has not been observed for porous media in the range of parameters spanned by the present study.

The vertical velocity profiles in the horizontal midplane displayed in Fig. 15 for N ranging from 2 to 15 (same parameters as previously, and $Da = 10^{-3}$), show the typical features of the flow in this range. First, as expected from the influence of the viscous term, the velocity is much smaller than in the Darcy regime. Then, the influence of the Brinkman term is such that the solutally and thermally driven flows merge together and that the influence of the thermal contribution in the buoyancy term is felt at much larger values of N than in the Darcy regime (Fig. 16).

5. CONCLUSION

The results presented in this paper show the main trends of thermosolutal natural convection in porous media. This contribution completes some observations on the Darcy regime already mentioned in previous studies. It brings out original results on the influence of the Darcy number when the Brinkman extension of the Darcy model is used.

It is shown that the numerical results for mass transfer are in excellent agreement with the scaling analysis over a very wide range of parameters. Heat transfer results show that boundary layer analysis is not suitable method to predict the correct scales for heat transfer in the same domain: as a conclusion of the analysis presented herein, it is clear that more investigation is required to derive the appropriate scaling laws in the domains where the flow is not fully dominated either by the thermal or by the solutal component of the buoyancy force.

This work also states the specific behavior of thermosolutal flows in porous media: first, the strong influence of the Darcy number on heat transfer is more complex than in thermal convection, and then the behavior of the thermosolutal flow in porous media is different from the behavior already assessed for fluids. The complete derivation of correlations showing the explicit influence of the Darcy number has still to be made.

The present analysis is focused on the influence of a limited number of dimensionless parameters: extensions of this work are presently developed particularly

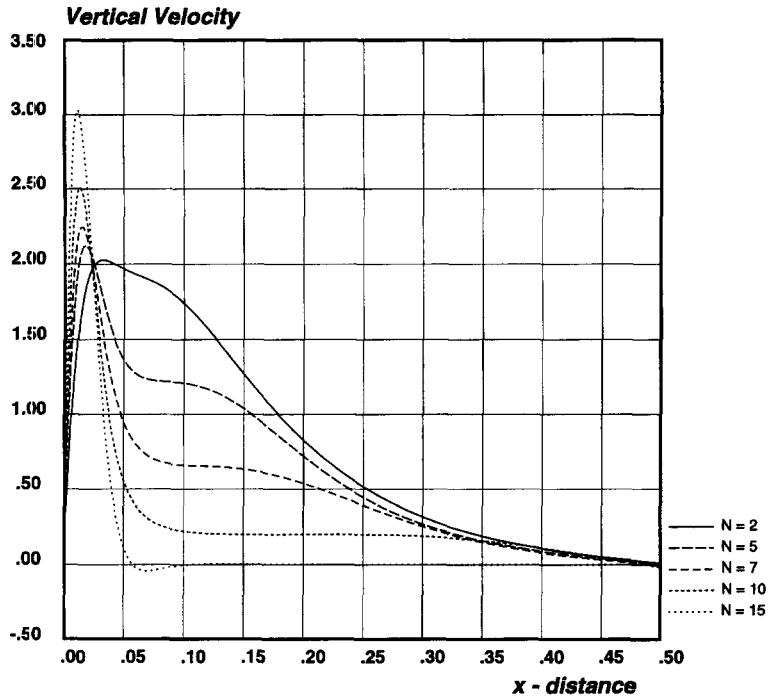

Fig. 15. Vertical velocity profiles in the horizontal midplane at $Da = 10^{-3}$ ($Ra^* = 100$; $Le = 100$; $A = 1$).

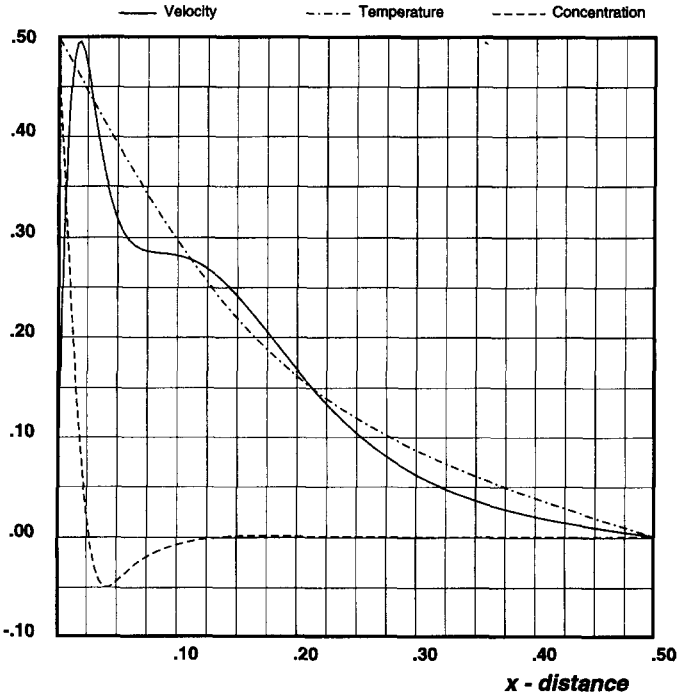

Fig. 16. Vertical velocity, temperature and concentration profiles in the horizontal midplane at $Da = 10^{-3}$ ($Ra^* = 100$; $Le = 100$; $A = 1$).

to analyze the influence of the aspect ratio in relation with the existence of multicellular regimes.

Acknowledgements— The calculations have been performed on the C98 Cray supercomputer of CNRS at IDRIS (Orsay), under grant 94-0336 of the Engineering Sciences Department of CNRS. This work was supported, in part, by CNES under grant 94-269. J.-P. Songbe's Thesis is supported by a research fellowship granted by MESR.

REFERENCES

1. D. A. Nield and A. Bejan, *Convection in Porous Media*. Springer, Berlin (1992).

2. D. A. Nield, Onset of thermohaline convection in a porous medium, *Water Resour. Res.* **4,** 553–560 (1968).
3. J. W. Taunton, E. N. Lightfoot and T. Green, Thermohaline instability and salt fingers in porous medium, *Phys. Fluids* **15,** 748–753 (1972).
4. H. Rubin, Onset of thermohaline convection in heterogeneous porous media, *Israel J. Technol.* **19,** 110–117 (1981).
5. N. Rudraiah, P. K. Srimani and R. Friedrich, Finite amplitude convection in a two-component fluid porous layer, *Int. J. Heat Mass Transfer* **25,** 715–722 (1982).
6. M. E. Taslim and U. Narusaw, Binary fluid composition and double-diffusive convection in a porous medium, *J. Heat Transfer* **108,** 221–224 (1986).
7. D. Poulikakos, Double-diffusive convection in a horizontal sparcely packed porous layer, *Int. Commun. Heat Mass Transfer* **13,** 587–598 (1986).
8. F. Chen and C. F. Chen, Double-diffusive fingering convection in a porous medium, *Int. J. Heat Mass Transfer* **36,** 793–807 (1993).
9. J. Y. Jang and W. J. Chang, The flow and vortex instability of horizontal natural convection in porous medium resulting from combined heat and mass buoyancy effects, *Int. J. Heat Mass Transfer* **31,** 769–777 (1988).
10. M. S. Malashetty, Anisotropic thermoconvective effects on the onset of double-diffusive convection in a porous medium, *Int. J. Heat Mass Transfer* **36,** 2397–2401 (1993).
11. D. A. Nield, D. M. Manole and J. L. Lage, Convection induced by inclined thermal and solutal gradients in a shallow horizontal layer of a porous medium, *J. Fluid Mech.* **257,** 559–574 (1993).
12. D. M. Manole, J. L. Lage and D. A. Nield, Convection induced by inclined thermal and solutal gradients, with horizontal mass flow, in a shallow horizontal layer of a porous medium, *Int. J. Heat Mass Transfer* **37,** 2047–2057 (1994).
13. B. J. Murray and C. F. Chen, Double diffusive convection in a porous medium, *J. Fluid Mech.* **201,** 147–166 (1989).
14. O. Trevisan and A. Bejan, Heat and mass transfer by high Rayleigh number convection in a porous medium heated from below, *Int. J. Heat Mass Transfer* **30,** 2341–2356 (1987).
15. N. D. Rosenberg and F. J. Spera, Thermohaline convection in a porous medium heated from below, *Int. J. Heat Mass Transfer* **35,** 1261–1273 (1992).
16. M. Mamou, P. Vasseur, E. Bilgen and D. Gobin, Double-diffusive convection in a shallow porous layer, *Proceedings of the 10th International Heat Transfer Conference* (1994).
17. G. Z. Gershuni, E. M. Zhukhovitskii and D. V. Lyubimov, Thermal concentration instability of a mixture in a porous medium, *Sov. Phys. Dokl.* **21**(7), 375–377 (1976).
18. G. Z. Gershuni, E. M. Zhukhovitskii and D. V. Lyubimov, Stability of stationary convective flow of a mixture in a vertical porous layer, *Fluid Dyn.* **15,** 122–127 (1980).
19. R. W. Griffiths, Layered double-diffusive convection in porous media, *J. Fluid Mech.* **102,** 221–248 (1981).
20. A. A. Khan and A. Zebib, Double-diffusive instability in a vertical layer of a porous medium, *J. Heat Transfer* **103,** 179–181 (1981).
21. A. Raptis, G. Tzivanidis and N. Kafousias, Free convection and mass transfer flow through a porous medium by an infinite vertical limiting surface with constant succion, *Lett. Heat Mass Transfer* **8,** 417–424 (1981).
22. A. Bejan and K. R. Khair, Heat and mass transfer by natural convection in a porous medium, *Int. J. Heat Mass Transfer* **28,** 909–918 (1985).
23. C. Allain, M. Cloitre and A. Mongruel, Scaling in flows driven by heat and mass convection in a porous medium, *Europhys. Lett.* **20,** 313–318 (1992).
24. F. C. Lai and F. A. Kulacki, Coupled heat and mass transfer by natural convection from vertical surfaces in porous media, *Int. J. Heat Mass Transfer* **34,** 1189–1194 (1991).
25. O. Trevisan and A. Bejan, Natural convection with combined heat and mass transfer buoyancy effects in a porous medium, *Int. J. Heat Mass Transfer* **28,** 1597–1611 (1985).
26. T. F. Lin, C. C. Huang and T. S. Chang, Transient binary mixture natural convection square enclosures, *Int. J. Heat Mass Transfer* **33,** 287–299 (1990).
27. T. F. Lin, Unsteady natural convection heat and mass transfer in saturated porous enclosure, *Wärme-und Stoffübertragung* **28,** 49–56 (1993).
28. O. Trevisan and A. Bejan, Heat and mass transfer by natural convection in a vertical slot filled with porous medium, *Int. J. Heat Mass Transfer* **29,** 403–415 (1986).
29. K. N. Metha and K. Nandakumar, Natural convection with combined heat and mass transfer buoyancy effects in non-homogeneous porous medium, *Int. J. Heat Mass Transfer* **30,** 2651–2656 (1987).
30. F. Alavyoon, On natural convection in vertical porous enclosures due to prescribed fluxes of heat and mass at the vertical boundaries, *Int. J. Heat Mass Transfer* **36,** 2479–2498 (1993).
31. F. Alavyoon, Y. Masuda and S. Kimura, On natural convection in vertical porous enclosures due to opposing fluxes of heat and mass prescribed at the vertical walls, *Int. J. Heat Mass Transfer* **37,** 195–206 (1994).
32. G. Lauriat and V. Prasad, Natural convection in a vertical porous cavity: a numerical study for Brinkman-extended Darcy formulation, *J. Heat Transfer* **109,** 688–696 (1987).
33. T. S. Lundgren, Slow flow through stationary random beds and suspensions spheres, *J. Fluid Mech.* **51**(2), 273–299 (1972).
34. R. C. Gilver and S. A. Altobelli, A determination of the effective viscosity for the Brinkman-Forchheimer flow model, *J. Fluid Mech.* **258,** 355–370 (1994).
35. S. V. Patankar, *Numerical Heat Transfer and Fluid Flow*. Hemisphere, New York (1980).
36. V. Prasad and F. A. Kulacki, Natural convection in a vertical porous annulus, *Int. J. Heat Mass Transfer* **27,** 207–219 (1984).
37. R. Bennacer, Convection naturelle thermosolutale: simulation numérique des transferts et des structures d'écoulement, Doctorat de l'Université Pierre et Marie Curie (1993).